RESEARCH ARTICLE

THE FASEB JOURNAL

Matrix stiffness primes lymphatic tube formation directed by vascular endothelial growth factor-C

Laura Alderfer[1] | Elizabeth Russo[2] | Adriana Archilla[3] | Brian Coe[2] |
Donny Hanjaya-Putra[1,2,3,4] (iD)

[1]Bioengineering Graduate Program, University of Notre Dame, Notre Dame, Notre Dame, IN, USA

[2]Aerospace and Mechanical Engineering, University of Notre Dame, Notre Dame, Notre Dame, IN, USA

[3]Notre Dame Nanoscience and Technology (NDnano), University of Notre Dame, Notre Dame, Notre Dame, IN, USA

[4]Chemical and Biomolecular Engineering, University of Notre Dame, Notre Dame, Notre Dame, IN, USA

Correspondence
Donny Hanjaya-Putra, Aerospace and Mechanical Engineering, University of Notre Dame, 141 Multidisciplinary Research Building, Notre Dame, IN 46556, USA.
Email: dputra1@nd.edu

Abstract

Dysfunction of the lymphatic system is associated with a wide range of disease phenotypes. The restoration of dysfunctional lymphatic vessels has been hypothesized as an innovative method to rescue healthy phenotypes in diseased states including neurological conditions, metabolic syndromes, and cardiovascular disease. Compared to the vascular system, little is known about the molecular regulation that controls lymphatic tube morphogenesis. Using synthetic hyaluronic acid (HA) hydrogels as a chemically and mechanically tunable system to preserve lymphatic endothelial cell (LECs) phenotypes, we demonstrate that low matrix elasticity primes lymphatic cord-like structure (CLS) formation directed by a high concentration of vascular endothelial growth factor-C (VEGF-C). Decreasing the substrate stiffness results in the upregulation of key lymphatic markers, including PROX-1, lymphatic vessel endothelial hyaluronan receptor 1 (LYVE-1), and VEGFR-3. Consequently, higher levels of VEGFR-3 enable stimulation of LECs with VEGF-C which is required to both activate matrix metalloproteinases (MMPs) and facilitate LEC migration. Both of these steps are critical in establishing CLS formation in vitro. With decreases in substrate elasticity, we observe increased MMP expression and increased cellular elongation, as well as formation of intracellular vacuoles, which can further merge into coalescent vacuoles. RNAi studies demonstrate that MMP-14 is required to enable CLS formation and that LECs sense matrix stiffness through YAP/TAZ mechanosensors leading to the activation of their downstream target genes. Collectively, we show that by tuning both the matrix stiffness and VEGF-C concentration, the signaling pathways of CLS formation can be regulated in a synthetic matrix, resulting in lymphatic networks which will be useful for the study of lymphatic biology and future approaches in tissue regeneration.

1 | INTRODUCTION

Lymphatic vasculature pervades the human body and is responsible for lipid transport, immune cell trafficking, extracellular fluid homeostasis, and inflammatory responses.[1,2] Consequently, the lymphatic system plays a crucial role in the progression of a wide spectrum of conditions, including congenital disorders, cancer and side-effects of cancer treatments, cardiovascular disease, diabetes, and parasitic infections.[3,4] Despite the significance of the lymphatic system and its consequences in numerous disease states, current treatments are limited to primitive and transient management solutions such as compression garments for lymphedema, or entirely absent for other lymphatic complications. Controlling the formation of new lymphatic vessels is postulated as an innovative therapeutic strategy for rescuing various disease phenotypes including metabolic syndrome, Alzheimer's, lymphedema, cardiovascular disease, and impaired wound healing.[2,5] Yet little is known about the molecular regulation that controls lymphatic cord-like structure (CLS) formation within a synthetic, in vitro system. Beyond conditions that arise from lymphatic dysfunction, a significant bottleneck for the field of tissue engineering is the vascularization of tissues and in vivo endothelial cell organization to form capillaries.[6,7] Promoting blood and lymphatic vascular networks within tissue-engineered constructs has been shown to improve their in vivo functionality.[8] However, a perennial challenge associated with this goal of controlling in vitro or in vivo morphogenesis of cellular structures includes the need to accurately replicate the morphology and cellular organization of lymphatic vessels.[6] To address this challenge, here, we utilize a synthetic matrix as a modular scaffold with tunable properties to control CLS formation.

Significant advances in therapeutic strategies that combine material engineering with biotechnological advances to promote vascular regeneration have occurred in recent decades.[9–11] Hydrogels have demonstrated success in in vitro applications for blood vasculature regeneration and provide promise for approaches to generate functional lymphatic capillaries.[11,12] Hyaluronic acid-based hydrogels (HA-hydrogels) have particularly shown great promise, either as a stand-alone therapy or as a scaffold to deliver molecules and cells.[13,14] Hyaluronan/hyaluronic acid (HA) is a nonsulfated linear polysaccharide of (1-β-4)d-glucuronic acid and (1-β-3)N-acetyl-d-glucosamine. HA is abundant during embryogenesis,[15] where it has a crucial role in regulating angiogenesis, lymphangiogenesis, and organ morphogenesis.[16,17]

HA is ubiquitous in the native ECM, nonimmunogenic, and able to be chemically modified, making HA widely used in tissue engineering and medicine.[13,18,19] HA also has an important function in maintaining homeostasis and biomechanical integrity of many organs.[20] In the lymphatic system, lymphatic endothelial cells (LECs) uniquely express lymphatic vessel endothelial hyaluronan receptor-1 (LYVE-1), a CD44 homologue, which is responsible for HA binding. LYVE-1 is expressed by LECs and serves as a unique binding receptor for HA.[21] LYVE-1 binding to HA presents the potential to use HA-hydrogels as a modular platform to study lymphatic vascular morphogenesis. By controlling ligand binding sites and mechanical properties, HA-hydrogels are investigated in these studies as a platform that can be engineered to generate robust and functional vascular networks from LECs. Overall, due to its developmental relevance, importance for LECs, and ability to support viable cells, HA-hydrogels are an excellent candidate biomaterial to control lymphatic CLS formation in a biomimetic environment.

Previous developmental biology studies have revealed that the transcription factor prospero-related homeobox 1 (PROX-1) initiates lymphatic sprouting and that the growth factor VEGF-C promotes the growth of lymphatic vessels.[22] Additionally, PROX-1 has been shown to be inversely regulated with the mechanosensitive proteins YAP and TAZ.[23] YAP/TAZ expression have extensively been reported to be influenced by substrate stiffness and provide an avenue of modulation in our HA hydrogel system. Another protein associated with lymphangiogenesis, VEGFR-3, has recently been discovered to be influenced by substrate stiffness,[24] which raises the potential to create biomaterials to promote expression of this key protein involved in the VEGF-C/VEGFR-3 signaling axis that is crucial for lymphangiogenesis.

Here, we utilize HA-hydrogels with defined composites and tunable elasticity for in vitro studies of lymphatic CLS formation. Viscoelasticity measurements demonstrate three distinct and physiologically relevant substrate stiffness profiles: firm, medium, and soft, which allow us to decouple the effects of matrix elasticity and ligand binding density. We first demonstrate that HA-hydrogels preserve key lymphatic markers, including PROX-1 and LYVE-1. Decreasing matrix stiffness results in upregulation of VEGFR-3, which primes LECs to form CLS in response to VEGF-C stimulation in vitro. RNAi studies demonstrate that MMP-14 is required to enable CLS formation and that LECs sense matrix stiffness through YAP/TAZ

mechanosensors. Collectively, we demonstrate that by tuning both the matrix stiffness and VEGF-C concentration, the signaling pathways of CLS formation in vitro can be regulated in a synthetic matrix, resulting in lymphatic networks which will be useful for the study of lymphatic biology and future approaches in lymphatic regeneration.

2 | MATERIALS AND METHODS

2.1 | Human LEC culture

Human LECs derived from the dermis of two adult donors (PromoCell, Heidelberg, Germany) were expanded and used for experiments between passages 5 and 9. Human LECs were grown in endothelial cell growth medium MV 2 (EGM MV2; PromoCell) and incubated at 37°C with 5% CO_2. Human LECs were characterized for the positive expression of CD31, LYVE-1, PROX-1, and podoplanin throughout the experiments. All cell lines were routinely tested for mycoplasma contamination and were negative throughout this study.

2.2 | Preparation of HA-hydrogels

Hyaluronic acid hydrogels (HyStem-HP, Advanced BioMatrix, Carlsbad, CA) were prepared by mixing 0.4% (w/v) thiol-modified HA conjugated with heparin with 0.4% (w/v) thiol-modified gelatin in a 1:1 volume ratio with 0.25%, 1%, and 2% (w/v) polyethylene glycol diacrylate (PEGDA) crosslinker in a 4:1 volume ratio to obtain soft, medium, and firm substrates, respectively. A range of stiffnesses, consistent with those reported in previous studies,[23–25] were screened in preliminary studies.[23–25] The conditions of 0.25%, 1%, and 2% PEGDA crosslinker resulted in the greatest differences and were therefore selected for this study. The hydrogel solution was cast in three milliliter syringes for rheology measurements and the images presented in Figure 1A, 4-well glass bottom dishes (Matsunami) for confocal imaging, 96-well tissue culture plates for gene expression and protein assays, and 16-well chamber slides for transmission electron microscopy. Hydrogels were incubated at 37°C with 5% CO_2 for 16–24 hours to achieve full cross-linking before use in experiments. By casting the prepolymer hydrogel solution directly in the wells that were used for each experiment, uniform surfaces were achieved.

2.3 | Hydrogel mechanical characterization

A rheometer with parallel plate geometry (8 mm in diameter; TA Instruments, New Castle, DE) was utilized for oscillatory shear measurements of the storage modulus (G′) as previously described.[25,26] Briefly, oscillatory time sweeps at 1 Hz frequency and a constant strain of 5% were performed for 1 min on three samples ($n = 3$) for firm, medium, and soft hydrogels to characterize the storage modulus of the hydrogels as a function of PEGDA concentration.[27,28] These strain and frequency parameters were selected in order to measure G′ in the linear viscoelastic regime.[29] Rheological measurements were performed at room temperature and ambient air conditions, as dehydration of the hydrogels was negligible during the short testing duration. The Young's modulus (matrix stiffness) was calculated by $E = 2G'(1 + v)$. HA-hydrogels can be assumed to be incompressible,[29] such that their Poisson's ratio (v) approaches 0.5 and the relationship becomes $E = 3G'$.

2.4 | Lymphangiogenesis assay

Human LECs were seeded on firm, medium, and soft hydrogels at a density of 100,000 cells/cm^2, which was consistent to our previous studies,[25,27] and cultured for 12 hours in EGM MV2 media supplemented with either 0.5 or 50 ng/mL recombinant human VEGF-C (R&D Systems). Images were acquired from the middle of each well ($n = 10$ per condition) at 4× using an inverted light microscope (ECHO Revolve, San Diego, CA). After an initial screening at time intervals of 3, 6, 9, 12, and 15 hours, the 12-h timepoint was determined to be the ideal endpoint for imaging as it not only allowed for differences between conditions to develop but also allowed for images to be captured before some tube contraction occurred.[25,26]

2.5 | Quantification of lymphatic cord-like structures (CLS)

One image field per construct from ten distinct constructs ($n = 10$), captured during the lymphangiogenesis assay, was analyzed using kinetic analysis of vasculogenesis (KAV), a custom plug-in for FIJI.[30] Ten parameters per image were quantified, and the tubes/node ratio and network area were selected to compare the degree of CLS formation on each substrate.

2.6 | LEC gene expression

To analyze the effect of HA-hydrogels on lymphatic phenotypes, LECs were seeded on firm and soft hydrogels, as well as tissue culture plastic, and cultured for 48 hours in EGM MV2 media. Similarly, to analyze for gene expression during lymphatic tube morphogenesis, LECs were cultured on firm, medium, and soft hydrogels for 48 hours

in EGM MV2 supplemented with 0.5 ng/mL or 50 ng/mL VEGF-C. The 48-h timepoint was selected to ensure that the signaling cascade in response to VEGF-C and mechanical stimulation was captured. Each biological replicate was created by pooling RNA from three individual wells to collect a sufficient amount of RNA. At least three biological replicates ($n = 3$) were collected per condition and analyzed with real-time qRT-PCR with triplicate readings as previously described.[27] RNA was reverse transcribed using a high-capacity cDNA reverse transcription kit (Thermo Fisher) according to the manufacturer's protocol. cDNA was then used with the TaqMan Universal PCR Master
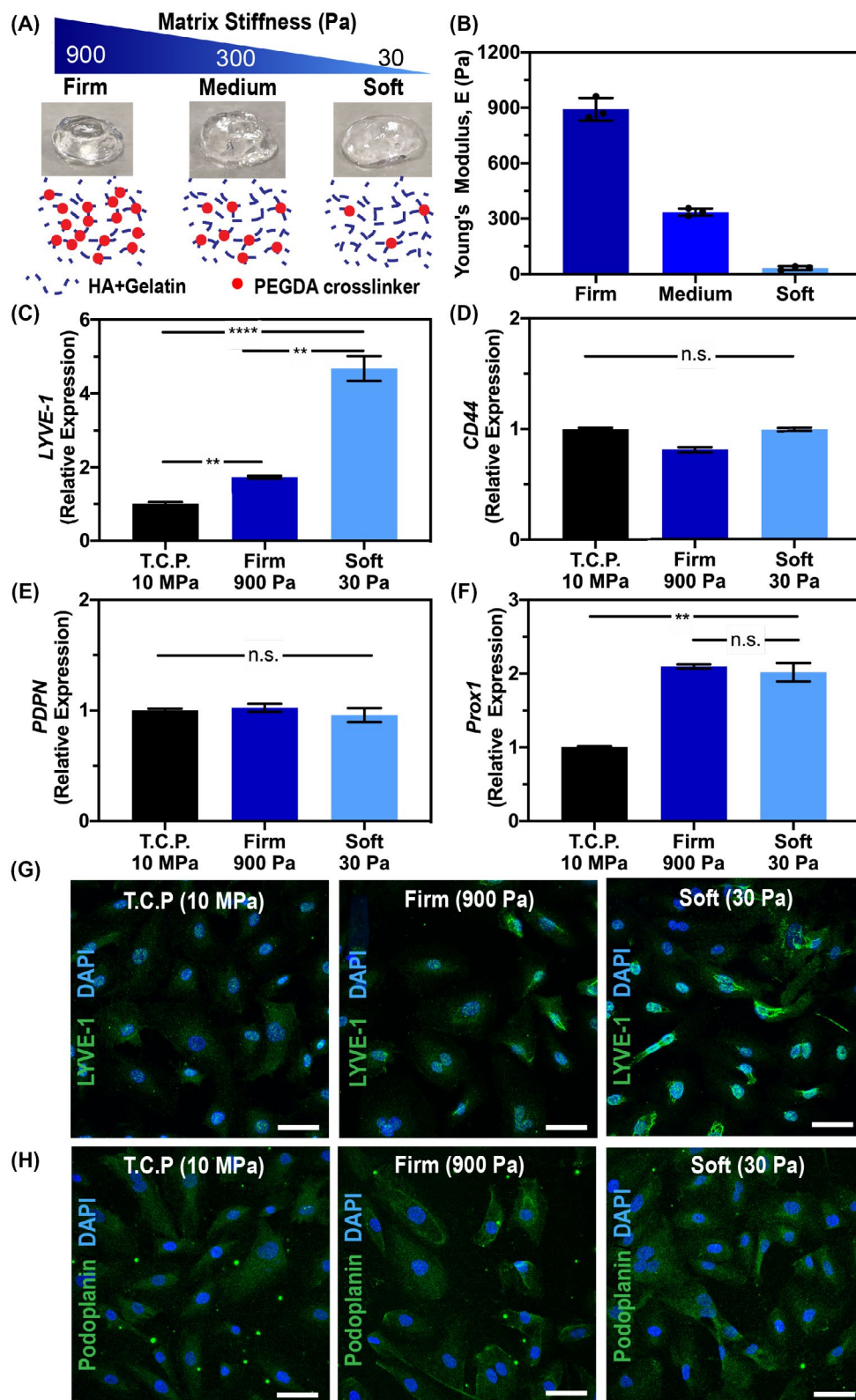
FIGURE 1 Tunable HA-hydrogels as a supportive matrix to preserve LEC phenotypes. A, Matrix elasticity of HA-hydrogels can be tuned with varying crosslinking density (*red* dots) without altering the polymer backbones (*blue* dotted lines). B, Rheological measurements of HA:gelatin in a 1:1 volume ratio with 2%, 1%, and 0.25% (w/v) of PEGDA crosslinker show three distinct profiles of hydrogel mechanics: firm, medium, and soft, respectively. Values shown are means ± S.D. of three independent hydrogel constructs. Please see Figure S1 for storage (G′) and loss (G″) modulus data. Real-time qRT-PCR data for key lymphatic markers (C) *LYVE-1*, (D) *CD44*, (E) *PDPN*, and (F) *PROX-1* expressed by LECs after being cultured on tissue culture plastic (E~10 MPa), firm (E~900 Pa), or soft (E~32 Pa) HA-hydrogels. Three biological replicates ($n = 3$) were collected per condition and analyzed with real-time qRT-PCR with triplicate readings. ANOVA followed by Tukey post hoc analysis was performed to analyze differences between substrate stiffnesses. Significance levels were set at: $^{n.s}P > .05$, $^{*}P < .05$, $^{**}P < .01$, and $^{***}P < .001$. Representative immunofluorescent images of LECs stained for (G) LYVE-1 and (H) podoplanin after being cultured on tissue culture plastic (E~10 MPa), firm (E~900 Pa), or soft (E~30 Pa) HA-hydrogels. Scale bars are 50 µm

Mix and Gene Expression Assays for *LYVE-1*, *PROX-1*, *CD44*, *Podoplanin*, *MMP-1*, *MMP-2*, *MMP-9*, *MMP-14*, *Flt4*, *YAP*, *TAZ*, *MYC*, *CTGF*, and *GAPDH* (Table S1). Each sample was prepared in triplicate, and the relative expression was normalized to *GAPDH* and analyzed using the $^{\Delta\Delta}$Ct method.

2.7 | Immunofluorescence

To analyze lymphatic protein expression, hLECs were seeded on firm and soft hydrogels, as well as tissue culture plastic, and cultured for 72 hours in EGM MV2 media. Samples were fixed with 3.7% formaldehyde, blocked with 1% BSA, permeabilized with 0.1% Triton-X, and stained for LYVE-1 and podoplanin (Table S2). To visualize lymphatic tube formation, hLECs cultured on hydrogels were fixed after 12 hours, and samples were incubated with their respective primary antibodies; Phalloidin, YAP, and TAZ. Samples were rinsed and then counterstained with DAPI. Phalloidin stained samples were imaged with a Lionheart Gen5 microscope (BioTek Instruments) and the z-series imaging modality. YAP and TAZ stained samples were imaged at 40× as a z-stack (Nikon A1R-MP Confocal microscope).

2.8 | Fluorescent intensity quantification

Confocal images of samples stained for YAP and TAZ were quantified for total fluorescent intensity using ImageJ (NIH). One field of view per sample was captured and a z-projection was created. Single cells in the field of view were quantified as individual samples. The fluorescent intensity in the nuclei and cytoplasm was gated and measured, and the background was then subtracted to give the corrected total cell fluorescence (CTCF).

2.9 | ELISA for VEGFR-3 protein quantification

Human LECs were seeded on firm, medium, and soft hydrogels and cultured in EGM MV2 media for 72 hours. A lysis buffer was used to isolate cells from the hydrogels, and cell lysates were analyzed using a Human VEGFR-3/Flt4 ELISA (R&D Systems, DY349B-05) kit according to the manufacturer's protocol.

2.10 | Transmission electron microscopy

Human LECs cultured on hydrogels for 6 and 12 hours were prepared for TEM samples as previously described.[25] Briefly, cells were fixed with 3.0% formaldehyde, 1.5% glutaraldehyde in 0.1 M Na cacodylate, 5-mM Ca^{2+} and 2.5% sucrose at room temperature for 1 hour and washed three times in 0.1 M cacodylate/2.5% sucrose pH 7.4 for 15 minutes each. The cells were postfixed with Palade's OsO$_4$ on ice for 1 hour, rinsed with Kellenberger's uranyl acetate and then processed conventionally through Epon embedding on a 16-well Lab-Tek chamber slide (NUNC). Serial sections were cut, mounted onto copper grids, and viewed using a Phillips EM 410 transmission electron microscope (FEI, Hillsboro, OR). Images were captured with a FEI Eagle 2k camera.

2.11 | RNAi transfection

Human LECs were transfected with siGENOME SMARTpool human *MMP-14* or human *PROX-1* (Dharmacon, Lafayette, CO) using the manufacturer's protocol. Human LECs were cultured to 90% confluency in 6-well plates with EGM MV2 media (PromoCell) and no additional VEGF-C supplementation. The RNAi transfection solution was prepared by mixing DharmaFECT2 RNAi transfection reagent (Dharmacon) with serum-free and antibiotic-free EGM MV2 media. To transfect the cells, EGM MV2 media was removed and replaced with 1.6 ml of antibiotic-free EGM MV2 and 400-µL transfection solution in each well to achieve a final RNAi concentration of 50 nM. Transfected cells were incubated at 37°C and 5% CO$_2$. After 72 hours, total RNA was isolated, and real-time qRT-PCR was performed, as described in the previous subsection, to confirm the knock-down of *MMP-14* or *PROX-1* expression.

2.12 | Statistical analysis

Statistical analysis was performed with GraphPad Prism (GraphPad Software Inc., La Jolla, CA). For each hydrogel condition, at least three independent experiments were performed with three technical replicates. Statistical comparisons were made using Student's t test for paired data, analysis of variance (ANOVA) for multiple comparisons, and with Tukey post hoc analysis for parametric data. Specifically, ANOVA followed by Tukey post hoc analysis was performed to analyze differences between substrate stiffness with the same VEGF-C concentrations, and Student's t test was used to analyze differences between low and high VEGF-C concentrations with the same substrate stiffness. Significance levels were set at the following: $^{*}P < .05$, $^{**}P < .01$, $^{***}P < .001$, $^{****}P < .0001$.

3 | RESULTS

### 3.1 | HA-hydrogels preserve LEC phenotypes

Because LECs uniquely express LYVE-1 to bind to HA and activate intracellular signaling to promote lymphangiogenesis,[21,31] we postulated that tunable HA-hydrogels can serve as a supportive matrix for lymphatic tube formation in vitro. Toward this goal, our initial investigations focused on studying the effect of HA-hydrogels and their mechanical influence on LEC phenotypes. Employing a similar method to our previous studies, where we have extensively characterized HA-hydrogels to control vascular tube morphogenesis,[25–28] we generated HA-hydrogels with varied crosslinker concentrations to mimic a wide range of physiologically relevant matrix stiffnesses, while preserving uniform presentation of cell adhesion molecules (Figure 1A). It is important to note that one advantage of synthetic HA hydrogels is that the chemistry of the polymeric networks is easily controlled via reaction conditions and is uniform between various batches,[13,32] which is difficult to impossible to achieve with naturally derived matrices, such as collagen and Matrigel.[33,34] Moreover, although enzymatic crosslinking of such natural gels as collagen and Matrigel allows studies of increased stiffness, it also results in increased protein concentration and ligand density, which make it difficult to decouple the effects of matrix stiffness from other matrix properties.[26,35]

For the present study, we utilized thiol-modified HA-gelatin hydrogels to study lymphatic cellular response to a wide range of tunable mechanical stimuli.[25,26,29] By varying PEGDA crosslinker concentrations (from 0.25% to 4%), while preserving the HA:gelatin ratio, hydrogels with a wide range of Young's moduli (matrix stiffness) were established (Figure S1). After our initial screening, we selected three crosslinker conditions that created hydrogels with distinct Young's moduli (E, matrix stiffnesses): firm (890 ± 61 Pa), medium (335 ± 20 Pa), and soft (32 ± 10 Pa) for our subsequent studies (Figure 1B). Next, we investigated the effect of HA-hydrogel matrix stiffness on key lymphatic markers that are uniquely expressed by LECs. Real-time qRT-PCR data revealed that LECs cultured on HA-hydrogels showed increased expression of *PROX-1* and *LYVE-1* compared to LECs cultured on plastic tissue culture plates, whereas expression of *CD44* and *PDPN* were relatively constant across different conditions (Figure 1C–F). Interestingly, the expression level of *LYVE-1* and *PROX-1* increased with decreasing matrix stiffness (Figure 1C,F). The soft matrix demonstrated the highest *PROX-1* (twofold increase) and *LYVE-1* (fivefold increase) expression, which is quite significant given that LECs are notoriously known to lose *LYVE-1* expression during in vitro culture[36] and therefore need to be cultured on fibronectin coated plates to maintain their lymphatic phenotypes.[37] Although *PROX-1* expression was elevated but constant on different hydrogel stiffnesses compared to tissue culture plates, *LYVE-1* expression was influenced by substrate stiffness and was greater on the soft hydrogels compared to the firm hydrogels. These observations regarding *LYVE-1* expression were also qualitatively confirmed using immunofluorescent imaging (Figure 1G). Although LYVE-1 is a CD44 homolog capable of HA binding,[21] we observed that decreasing the matrix stiffness of HA hydrogels effected *LYVE-1* but not *CD44*. *PDPN* expression, a membrane marker of LECs, was also not altered by changes in matrix stiffness (Figure 1E,H). Collectively, these results underscore the enhanced ability of HA-hydrogels to preserve LEC phenotypes which is an important enabling step towards utilizing tunable HA-hydrogels to control lymphatic tube formation in tissue engineering approaches.

3.2 | Effect of VEGF-C and matrix stiffness on CLS formation

High concentrations of VEGF-C (ie, 50 ng/mL) were previously demonstrated to induce differentiation into LECs,[38] as well as lymphangiogenesis in both in vitro and in vivo models.[39,40] Therefore, to study CLS formation in a controllable in vitro system, we seeded human LECs on HA hydrogel substrates and cultured them for 12 hours in media supplemented with either 0.5 ng/mL (low) or 50 ng/mL (high) VEGF-C. We observed minimal branching of LECs seeded on the firm hydrogels supplemented with low VEGF-C (data not shown) or even with high VEGF-C (Figures 2A and S2). Conversely, when LECs were seeded on soft hydrogels with only 0.5-ng/mL VEGF-C, the mechanical environment allowed some cellular branching to occur (Figure S3). Moreover, CLS formation on soft hydrogels was further enhanced with a higher VEGF-C supplementation, leading to greater network areas
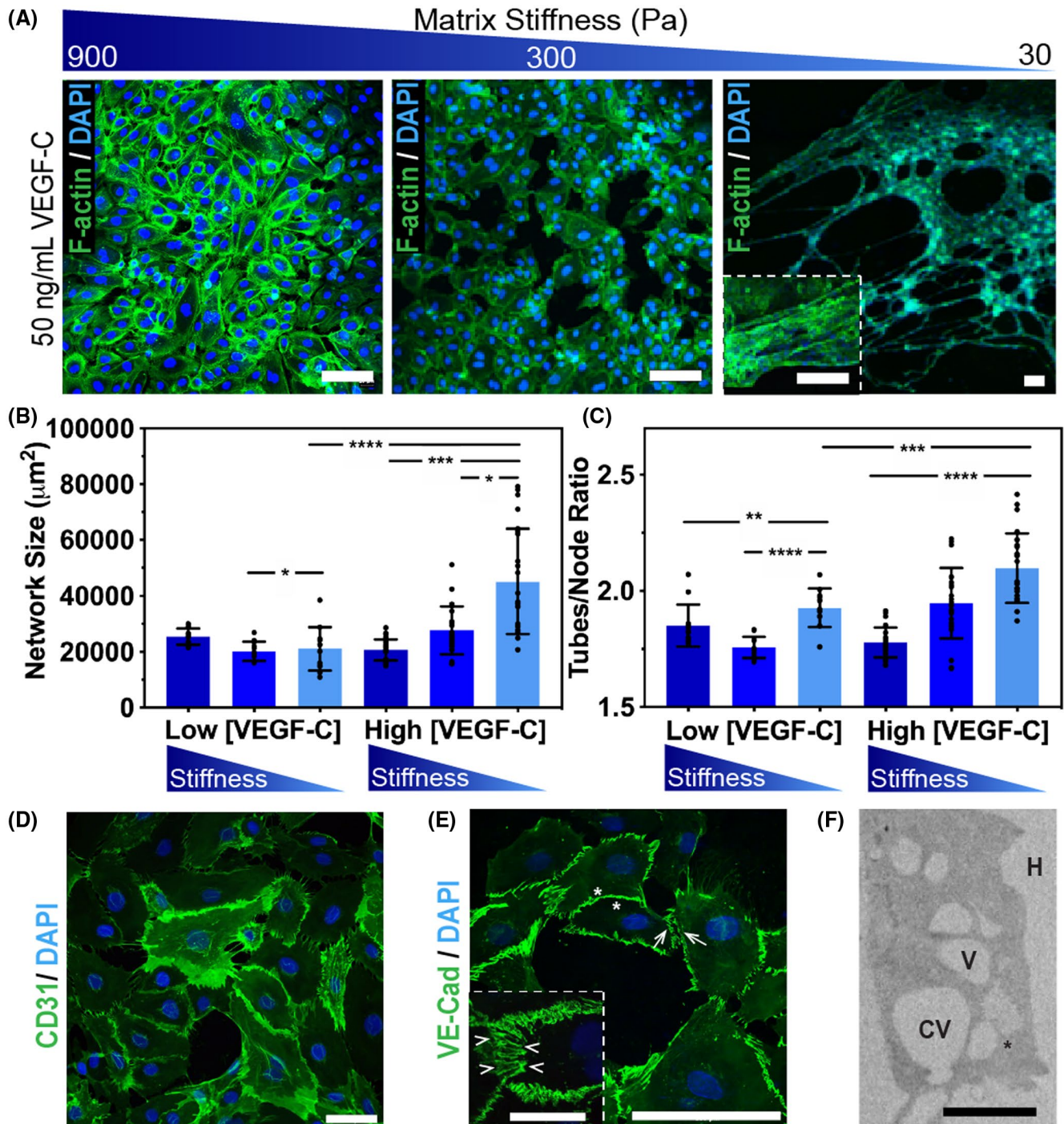
FIGURE 2 VEGF-C and matrix stiffness regulate lymphatic cord-like structure formation. A, Human LECs were seeded on firm, medium, and soft substrates for 12 hours supplemented with 50-ng/mL VEGF-C and formed CLS, as demonstrated by fluorescence microscopy of F-actin (green) and nuclei (blue). Scale bars are 50 μm. B, Kinetic analysis of vasculogenesis (KAV) revealed a significant increase in network size and C, tubes/node ratios as substrate stiffness decreased. Data represents the mean ± S.D. of 10 biological replicates performed. Confocal images of CLS formed on soft substrates showing junctional markers D, CD31 and E, VE-Cad. Enlarged rendering of the confocal image stack indicates cellular junctions (arrowheads) with discontinuous (arrows) and overlapping (asterisks) junctions. F, TEM analyses of CLS formed after 12 hours showed LECs degrading the hydrogels H, to generate intracellular vacuoles (V), some of which were observed in the process of merging (asterisk) into coalescent vacuoles (CV). ANOVA followed by Tukey post hoc analysis was performed to analyze differences between substrate stiffness within the same VEGF-C concentrations, and Student's t test was used to analyze differences between low and high VEGF-C concentrations for the same substrate stiffness. Significance levels were set at $^*P < .05$, $^{**}P < .01$, $^{***}P < .001$, $^{****}P < .0001$. Scale bars are (A) 50 μm; (D) 50 μm; (E) 50 μm, and 25 μm (inset); and (F) 20 μm

and a higher extent of branching (Figure 2A), demonstrating that given the right mechanical environment, VEGF-C can amplify CLS formation in vitro.

Next, we utilized the kinetic analysis of vasculogenesis (KAV) Fiji plug-in to quantitate lymphatic tube formation and provide high-throughput lymphangiogenic analysis (Figure S4).[30,41] Quantification reveals that substrate stiffness influences LEC network assembly and decreasing matrix elasticity results in a significant increase in lymphatic network size—from $(20.7 \pm 3.8) \times 10^3$ μm^2 on firm substrates to $(27.7 \pm 8.6) \times 10^3$ μm^2 on medium substrates to $(44.0 \pm 8.4) \times 10^3$ μm^2 on soft substrates (Figure 2B). Similarly, the tubes/node ratio, or the extent of branching, also increased—from 1.78 ± 0.07 on firm substrates to 1.99 ± 0.13 on medium substrates to 2.08 ± 0.13 on soft substrates (Figure 2C). It should be noted that although the network structures in Figure 2A are slightly less extensive than the networks shown in Figures S2 and S3, the differences resulted from the networks being perturbed during the immunostaining process and did not arise during the tube formation process. Phase contrast images like the ones presented in Figure S3 were used for quantification with KAV, and immunofluorescence images were used for cytoskeleton visualization.

Very limited CLS formation occurred on firm and medium substrates supplemented with 50 ng/mL VEGF-C, whereas extensive lymphatic tubes, similar to the tubes formed when LECs were seeded on Matrigel,[42] formed on the soft substrates supplemented with 50-ng/mL VEGF-C (Figure 2A–C). Moreover, to study cellular junctions formed on the soft substrates, we stained CLS with CD31 and VE-Cadherin as junctional markers (Figure 2D,E). Using confocal analysis and 3D rendering, we observed lymphatic CLS with discontinuous and overlapping junctions (Figure 2E). To further confirm these observations and investigate the cell-matrix interactions that facilitate the formation of intracellular vacuoles, TEM analysis was performed following our previously published protocols.[25,27] After 12 hours of culture, LECs on soft substrates were found elongated and degrading the hydrogels to form intracellular vacuoles (Figure 2F). Some of these intracellular vacuoles were in the process of merging into coalescent vacuoles, which is consistent with the tunneling model of lymphatic vessel formation observed in other in vitro and in vivo models of lymphatic vessel formation.[43,44]

3.3 | Matrix stiffness primes LECs for VEGF-C induced lymphatic tube formation in vitro

To examine how matrix elasticity and high concentrations of VEGF-C would coregulate lymphatic tube formation in vitro, our initial investigations focused on the expression of VEGFR-3, also known as Flt4. Real-time qRT-PCR indicates

that decreasing matrix stiffness correlated with an increase in *VEGFR-3* expression by LECs cultured with either low or high concentrations of VEGF-C (Figure 3A). Interestingly, this trend seemed to be influenced by matrix stiffness and not VEGF-C concentrations. This trend was also confirmed via ELISA to detect the presence of total VEGFR-3 expressed by LECs (Figures 3B and S5A). These findings suggest that softer matrices, in particular the soft substrate, primes the LECs to express more VEGFR-3, which enables effective stimulation of LECs with VEGF-C.

Next, we investigated how stimulation with VEGF-C would induce MMP expression to enable cell migration, which is a crucial step in enabling lymphatic tube formation. Real-time qRT-PCR was performed to compare MMP expression in LECs cultured on firm, medium, and soft substrates supplemented with 50-ng/mL (high) VEGF-C versus with 0.5-ng/mL (low) VEGF-C (Table S1 and Figure S5B). After 48 h of incubation in media supplemented with high VEGF-C, LECs showed increased production of *MMP-1*, *-2*, and *-14*. The increase in MMP production became more significant for LECs cultured on the soft substrate (Figure 3C–E). Specifically, LECs cultured on soft substrates with high VEGF-C produced two times the *MMP-2* (Figure 3D) and three times the *MMP-14* (Figure 3E) produced by LECs cultured in media supplemented with low VEGF-C. The increase in MMP expression that correlates with the decrease in matrix stiffness is very intriguing, especially given the importance of MMPs in regulating lymphatic tube formation.[45] In particular, MMP-14 can activate pro-MMP-2 to localize MMP activity at the direction of cell migration, which is responsible in the formation of lumen compartments.[44,46] This result highlights the importance of MMP-1, -2, and -14 during lymphatic tube formation, particularly in the soft substrates. Collectively, these findings suggest that matrix elasticity primes LECs to express VEGFR-3 on the cell surface, which in turn enables effective VEGF-C stimulation and increased expression of MMPs to form lymphatic tube networks in vitro.

3.4 | YAP/TAZ are mechanosensors of matrix stiffness in LECs

To investigate the effect of matrix elasticity on in vitro lymphatic tube formation, we focused our investigation on the Hippo pathway YAP/TAZ, which are known as sensors and mediators of mechanical cues. YAP/TAZ are highly enriched in blood ECs of growing blood vessels and play crucial roles in angiogenesis by regulating cytoskeletal arrangement, proliferation, and cell motility.[47,48] More recently, the roles of YAP/TAZ in lymphatic vessel morphogenesis during development have been elucidated in mice and zebrafish.[23,49] Here, we demonstrate that the expression of YAP/TAZ by
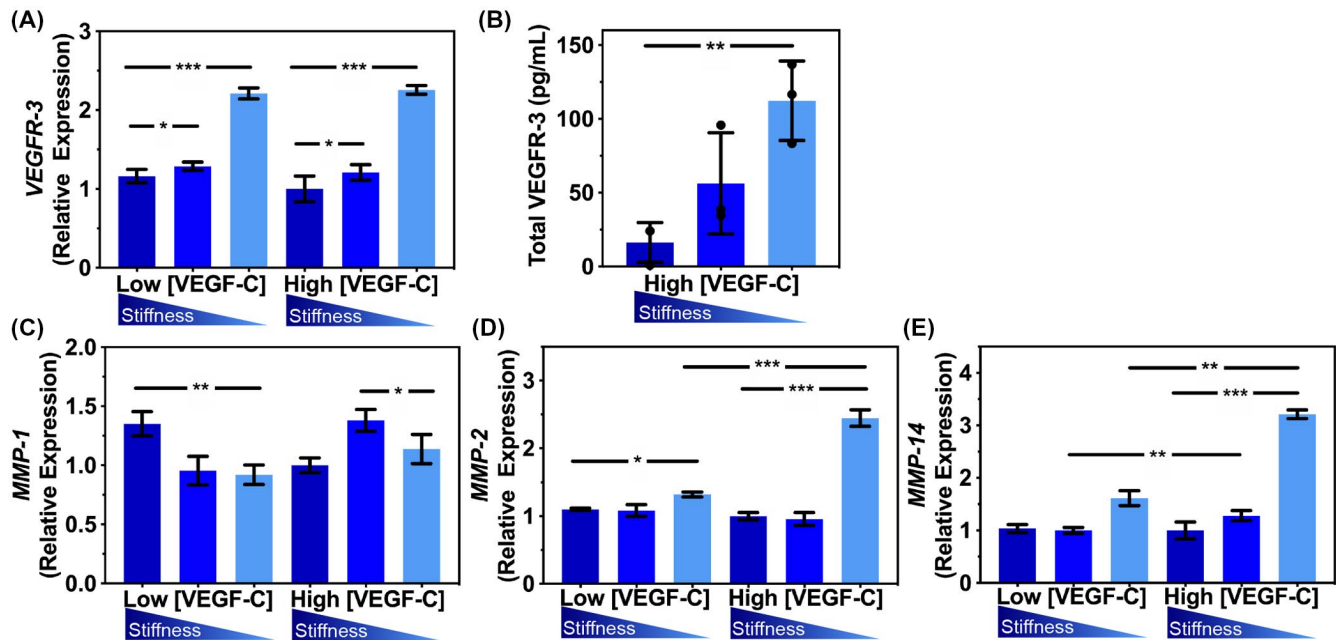
FIGURE 3 Expression of MMP-2 and MMP-14 is dependent on VEGF-C concentration and matrix stiffness. A, Real-time qRT-PCR data for *VEGFR-3* expressed by LECs after being cultured on firm, medium, or soft hydrogels for 48 hours. Three biological replicates ($n = 3$) were collected per condition and analyzed with real-time qRT-PCR with triplicate readings. B, ELISA analysis of soluble total VEGFR-3 secreted by LECs cultured on firm, medium, or soft hydrogels for 72 hours. Real-time qRT-PCR data for *MMP-1* (C), *MMP-2* (D), and *MMP-14* (E) show mRNA expression of MMP-1, MMP-2, and MMP-14 increases with decreases in matrix stiffness. Values shown are means ± S.D. from three independent experiments ($n = 3$) performed with three technical replicates. ANOVA followed by Tukey post hoc analysis was performed to analyze differences between substrate stiffnesses with the same VEGF-C concentrations, and Student's *t* test was used to analyze differences between low and high VEGF-C concentrations with the same substrate stiffness. Significance levels were set at $^{*}P < .05$, $^{**}P < .01$, $^{***}P < .001$

LECs during CLS formation in HA-hydrogels is regulated by matrix stiffness. Real-time qRT-PCR reveals that decreased matrix stiffness results in decreased *TAZ* expression but a nonsignificant decrease in *YAP* expression (Figure 4A,B), which led us to investigate their downstream targets *MYC* and *CTGF*, as well as *Prox-1* (Figure 4C–E). As matrix stiffness decreases, *MYC* and *CTGF* decrease to 0.33-fold and 0.5-fold, respectively. On firm substrates, YAP/TAZ enters the nucleus and binds to the PROX-1 promoter which inhibits transcription of PROX-1 and its targets, such as VEGFR-3 and MMP-14.[23,50] With decreasing matrix elasticity, YAP/TAZ are translocated into the cell membrane, leading to their cytoplasmic degradation (Figure 4F–H). Furthermore, decreasing matrix elasticity results in decreased nuclear localization of YAP and increased cytoplasmic localization of TAZ (Figure 4I,J). Subsequently, cytoplasmic degradation of YAP/TAZ enhances the transcription of PROX-1 (Figure 4E), including its targets VEGFR-3 and MMP-14 which are highly expressed on LECs cultured on the soft substrate with high concentrations of VEGF-C. It is important to note that although the soft matrix promotes expression of VEGFR-3, that trend does not occur for PROX-1 in the case of low VEGF-C supplementation (Figure S6) and may explain the limited CLS formed on soft matrices with low VEGF-C. Overall, these observations suggest the roles of YAP/TAZ as

mechanosensors of matrix stiffness to enable lymphatic tube formation in vitro through transcription of PROX-1, including its targets VEGFR-3 and MMP-14.[23,50]

3.5 | MMP-14 and PROX-1 are required for in vitro lymphatic tube formation

MMP-14, which is also known as MT1-MMP, has been reported to support blood vascular morphogenesis by allowing matrix degradation at the migrating cell front,[46] as well as by creating a vascular guidance tunnel to control lumen formation.[44] Recent evidence suggests that MMP-14 plays a crucial role in lymphatic formation during development and lymphatic metastasis.[24,51,52] We utilized an siRNA suppression approach to investigate the function of MMP-14 in lymphatic tube formation in soft substrates cultured with a high concentration of VEGF-C, where CLS formation was found to be optimized. LECs treated with siRNA targeting MMP-14 showed a significant decrease in MMP-14 expression compared to LECs treated with the Luciferase nontargeting control (Figure 5Ai). In contrast to the Luciferase-treated LECs (control), siRNA suppression of MMP-14 abrogated lymphatic tube formation on the soft substrates, with more rounded cell morphology (Figure 5B). KAV analysis indicates a reduction
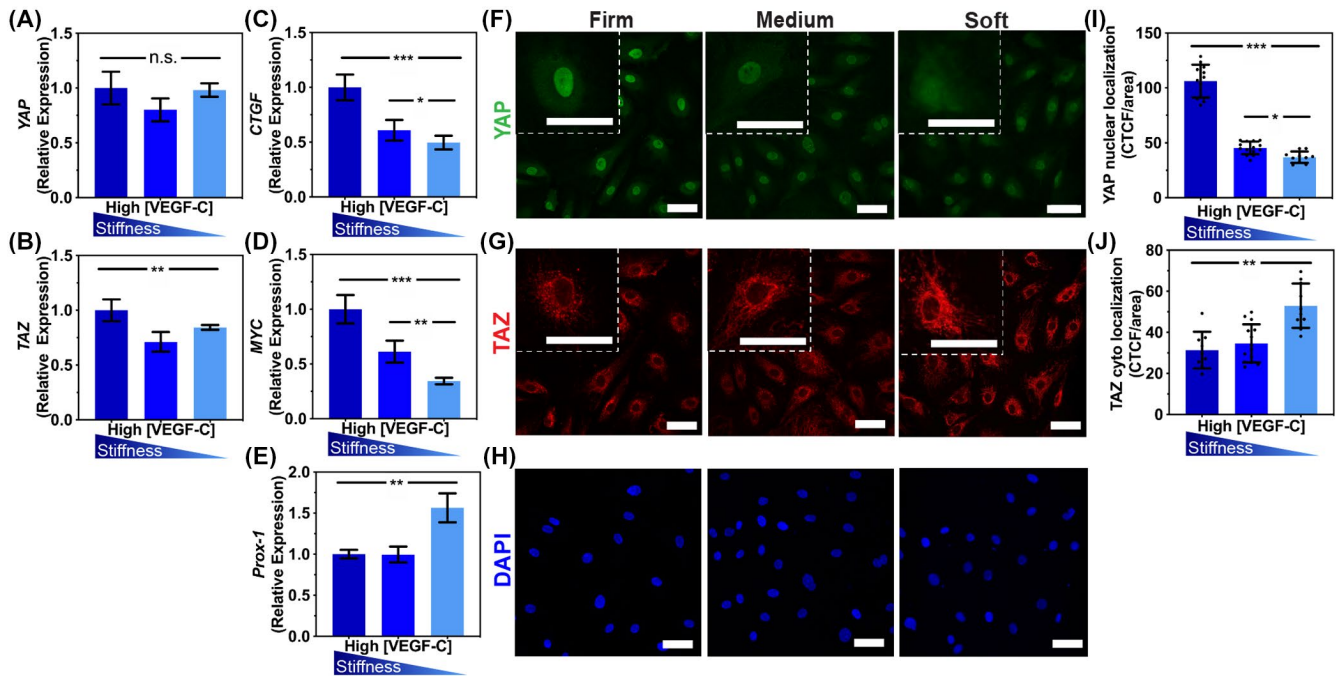
FIGURE 4 Mechanical regulation of lymphatic cord-like structure formation. Real-time qRT-PCR data for (A) *YAP*, (B) *TAZ* (C), *CTGF*, (D) *MYC,* and (E) *PROX-1* expressed by LECs after being cultured on firm, medium, or soft hydrogels supplemented with high VEGF-C (50 ng/mL) for 48 hours. Three biological replicates ($n = 3$) were collected per condition and analyzed with real-time qRT-PCR with triplicate readings. Confocal microscopy z-stacks of (F) YAP (green), (G) TAZ (red), and (H) nuclei (blue) indicate the localization of YAP/TAZ in lymphatic networks formed on the firm, medium, and soft hydrogels. Scale bars are 50 μm. Fluorescent intensity quantification demonstrates (I) a decrease in nuclear localization for YAP and (J) and an increase in cytoplasmic localization of TAZ as matrix stiffness decreases. CTCF, corrected total cell fluorescence. Values shown are means ± S.D. ANOVA followed by Tukey post hoc analysis was performed to analyze differences between substrate stiffnesses. Significance levels were set at: $^{n.s}P > .05$, $^{*}P < .05$, $^{**}P < .01$, $^{***}P < .001$

in network size of CLS formed in the siMMP-14 group compared to the siLuciferase control (Figure 5C).

Our next investigation focused on the role of PROX-1 in regulating lymphatic tube formation in response to matrix elasticity. A previous study reported that YAP/TAZ negatively regulate PROX-1 during lymphatic development.[23] We utilized an siRNA suppression approach to examine whether PROX-1 is the connecting link by which LECs respond to substrate stiffness during lymphatic tube formation. LECs treated with siRNA targeting PROX-1 showed a significant decrease in PROX-1 expression compared to LECs treated with the Luciferase nontargeting control (Figure 5Aii). In contrast to the Luciferase-treated LECs (control), siRNA suppression of PROX-1 mitigated lymphatic tube formation on the soft substrates, with more elongated cell morphology (Figure 5B). KAV analysis indicates a reduction in network size of CLS formed in the siProx-1 group compared to the siLuciferase control (Figure 5C). It is important to note that when siLuciferase, siMMP-14, or siProx-1 treated LECs were cultured on firm and medium substrates, they maintained a cobblestone morphology on monolayer culture with no indication of CLS formation (Figure S7). Collectively, these observations suggest that both MMP-14 and PROX-1 are required for matrix stiffness primed lymphatic tube formation induced by VEGF-C.

4 | DISCUSSION

LECs express LYVE-1, a specific receptor for HA, and provide a unique advantage for engineered matrices containing HA. We show that matrix stiffness and VEGF-C coregulate lymphatic tube formation. High levels of VEGF-C are required to initiate CLS formation, as well as activate MMPs to enable LEC migration. Under these conditions, substrate elasticity affects the progression of CLS formation. With decreases in substrate stiffness, we observe increased expression of *PROX-1* and activation of *VEGFR-3*, as well as cytoplasmic degradation of YAP/TAZ and downregulation of YAP/TAZ target genes. Furthermore, MMP-14 is required to enable the movement of LECs on the matrix and YAP/TAZ act as plastic regulators of lymphatic tube formation through PROX-1 transcriptional programming.

A chronic challenge of in vitro culture methods for lymphatic vasculature research is that LECs quickly lose their LEC-specific gene and protein expression.[37,53] Previous studies have shown that culturing LECs on fibronectin improved cell adhesion and proliferation, which highlights the critical signaling contribution that the culture substrate provides.[37] Here, we show that HA-hydrogels not only protect but improve LEC-specific markers and provide a
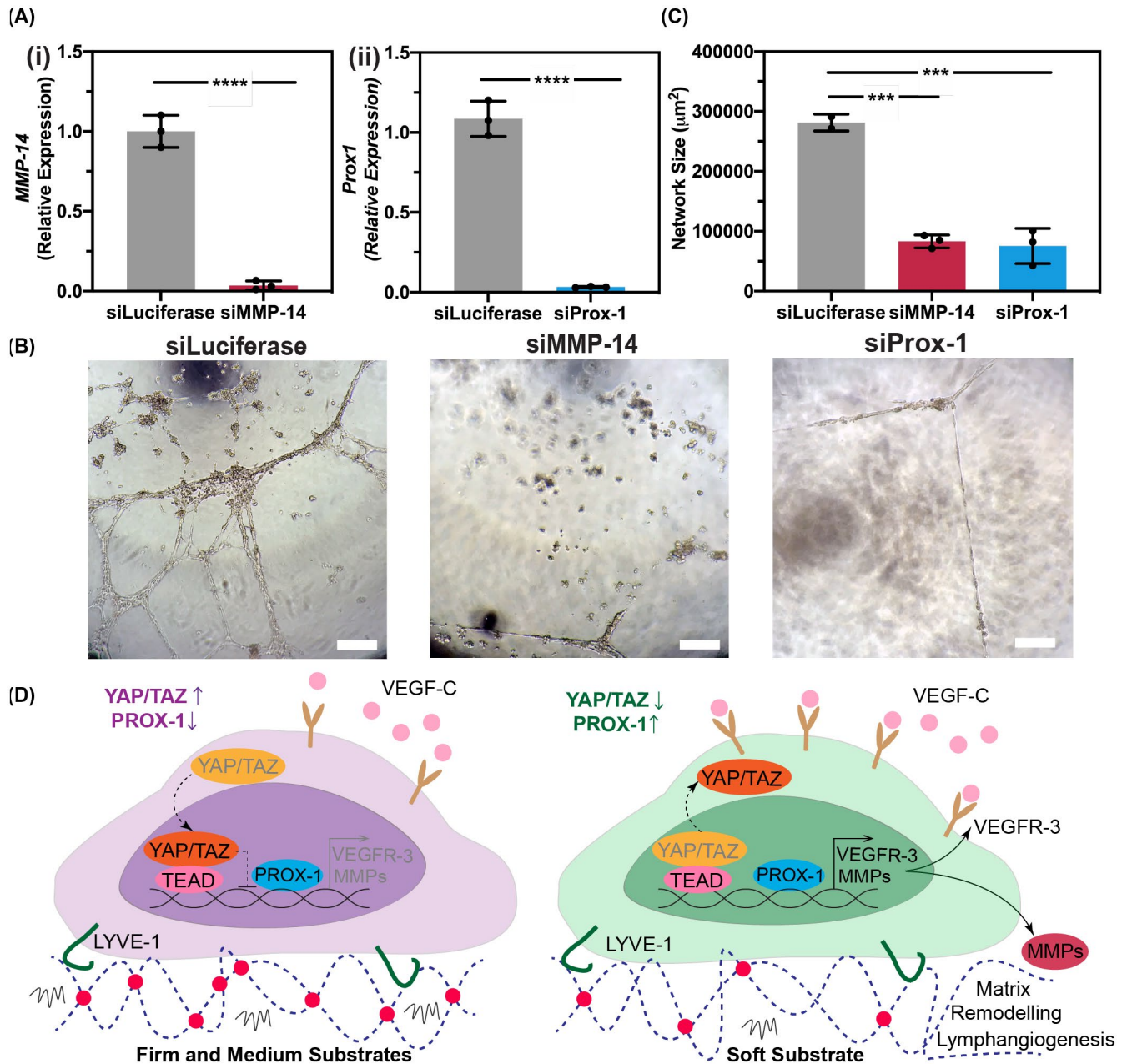
FIGURE 5 MMP-14 and Prox-1 are required for lymphatic cord-like structure formation. A, Human LECs transfected with siRNA for (*i*) *MMP-14* or (*ii*) *Prox-1* demonstrated a significant reduction in their expression for *MMP-14* or *Prox-1*, respectively, compared to non-targeting control (siLuciferase). Three biological replicates (*n* = 3) were collected per condition and analyzed with real-time qRT-PCR with triplicate readings. Statistical significance was assessed using Paired Student's *t* test. Significance levels were set at [****]*P* < .0001. B, Human LECs transfected with either siLuciferase, siMMP-14, or siProx-1 were seeded on the soft substrates and supplemented with 50-ng/mL VEGF-C for 12 hours. Scale bars are 50 μm. C, Kinetic analysis of vasculogenesis (KAV) revealed a significant reduction in network size in siMMP-14 and siProx-1 treated groups compared to the siLuciferase control. Data represent the mean ± S.D. of three biological replicates performed. Statistical significance was assessed using Paired Student's *t* test to analyze differences between RNAi-treated groups and the Luciferase control. Significance levels were set at [***]*P* < .001. D, Schematic diagram depicting the role of matrix elasticity in priming lymphatic tube formation directed by VEGF-C. HA-hydrogels were able to preserve key lymphatic markers, including LYVE-1. When LECs are cultured in firm and medium substrates, YAP/TAZ enter the nucleus and bind to the PROX-1 promoter, inhibiting its transcription, including its targets, such as VEGFR-3 and MMPs. However, decreasing matrix stiffness further primes LECs and enables YAP/TAZ to undergo cytoplasmic degradation, which subsequently enhance transcription of PROX-1, including its targets, such as VEGFR-3 and MMPs. Consequently, high MMP expression and binding of VEGF-C to VEGFR-3 results in matrix remodeling and lymphatic tube formation in vitro

more suitable in vitro system. Both *LYVE-1* and *PROX-1* expression increased in LECs cultured on HA-hydrogels versus plastic tissue culture plates, which highlights a possible strategy for promoting lymphatic-like behavior for more accurate in vitro mechanistic studies. Additionally, the design of this HA-hydrogel system allows mechanical and biochemical signals to be decoupled to probe the effects of their individual contributions. Although previous studies have been able to generate preliminary lymphatic vessels in fibrin,[8,54,55] collagen,[8] and Matrigel,[42,56] these hydrogel systems are limited due to both the mechanical and biochemical signaling being altered by any modifications to the system. If these materials are diluted in order to decrease the substrate stiffness, integrin binding sites and other crucial signaling factors are also diluted.[25,34] Here, our HA-hydrogel system can mechanically be altered by adjusting only the concentration of the PEGDA crosslinker which allows the substrate composition and ligand density to remain constant for all conditions. By using fully defined components in this HA-hydrogel system, we are also able to study the specific effects of VEGF-C in our system without the noise of additional growth factors that are sometimes included in other in vitro culture systems.

Another important characteristic of this HA-hydrogel system is the ability to generate a range of physiologically relevant substrate stiffnesses. During development, LECs migrate from the cardinal vein which has a Young's modulus of 3.6 kPa to the surrounding tissue which has a Young's modulus of only 270 Pa.[24] This transition to a significantly lower substrate stiffness highlights the need for softer substrates in order to recapitulate in vivo conditions for lymphangiogenesis. Previous studies have used hydrogels to study lymphatic vessel development, and although those hydrogel systems are advantageous compared to traditional tissue culture plastic culture methods, those systems still have Young's moduli on the scale of kPa to MPa.[24] Here, our modular hydrogel system has been tuned to have Young's moduli between 30 and 900 Pa (Figure 1A), representing the range of stiffnesses from the human brain to slightly stiffer than the surrounding tissue measured outside of the cardinal vein.[24] It is important to note that although we found that LECs are sensitive to these three substrate stiffness profiles in our HA-hydrogel system, they are still considered in the softer range of substrate stiffness profiles, and the sensitivity of substrate stiffness may be unique to the chosen hydrogel system. Nonetheless, these findings highlight the importance of a relatively softer substrate to support lymphatic phenotypes and CLS formation, which is also consistent with previous reports using other hydrogel systems.[23,24]

By decoupling the mechanical and biochemical effects, we show in these studies that the mechanical environment primes LECs for lymphangiogenesis and subsequently, VEGF-C promotes branching. Even with the supplementation of 50 ng/mL VEGF-C, only minimal branching occurs on the firm hydrogels (Figure 2C). Conversely, when LECs were seeded on soft hydrogels with only 0.5-ng/mL VEGF-C, the mechanical environment allowed rudimentary branching to occur (Figure S2). The CLS formation on soft hydrogels was further enhanced with a higher VEGF-C supplementation (Figure 2B,C), demonstrating that VEGF-C can amplify tube formation, but only if the mechanical environment is suitable. Additionally, our HA-hydrogel model has demonstrated that VEGFR-3 expression is predominantly controlled by the mechanical environment and supplementation of VEGF-C alone cannot induce increased VEGFR-3. This dependency on substrate stiffness also highlights a potential strategy to tune VEGFR-3 expression for specific applications. Collectively, these observations show that although VEGF-C does promote lymphangiogenesis, as extensively reported,[39,57] the mechanical environment is also critical for accurate in vitro models.

Beyond tuning VEGFR-3 expression, modifications to the substrate stiffness also modified MMP -1, -2, and -14 expression. MMP-14 is a cell surface activator of MMP-2,[58] and we observe mimetic trends in real-time qRT-PCR results for *MMP-2* and *MMP-14*. Although this trend was observed at the mRNA level and may not directly translate to protein expression of active MMPs,[27,28] our finding was consistent with previous reports. Previous studies have revealed the crucial role of MMP-2 in LEC tube formation, where knocking-down MMP-2 inhibited LEC migration through collagen gels and MMP-2 knockdown in zebrafish caused lymphatic defects.[45] MMP-2 degrades gelatin, which is contained in our HA-hydrogel system, allowing for LEC migration and branching, and supports our observed trend of increased MMP-2 expression corresponding with increased LEC branching and tube length. On the other hand, although expression of *MMP-1* also increased, the trend was not as significant as *MMP-2* and *MMP-14*. Because *MMP-1* degrades collagen, which is not a major component of our hydrogel system, these observations suggest that LECs can adapt to secrete specific MMPs depending on their microenvironment. Additionally, increased VEGFR-3 expression on softer matrices and increased binding with VEGF-C may also contribute to this upregulation of MMP-2 and MMP-14 to promote matrix remodeling and allow for the increased LEC tube formation that is observed. Furthermore, MMP-2 but not MMP-9 has been shown to impact LEC sprouting[45] and we observed substantially lower expression levels of MMP-9 compared to MMP-14 and MMP-2 in our screening run (Figure S5B). High expression of MMPs is also responsible for cellular elongation and hydrogel degradation to facilitate the formation of intracellular vacuoles and coalescent vacuoles as precursors to open lumen compartments, as observed in other in vitro and in vivo models of lymphatic vessel formation.[43,44] These supporting trends in our HA-hydrogel system with previous in vitro and in vivo studies regarding MMPs highlight the ability of our system

to accurately recapitulate the native environment that LECs sprout in. Furthermore, this evidence demonstrates that our HA-hydrogel system serves as a novel system that can be utilized for further mechanistic studies in a highly controllable environment.

In addition to *VEGFR-3* expression and PROX-1 being modulated by substrate stiffness, we also show that YAP/TAZ are important mechanosensitive proteins and transcription factors that contribute to regulating lymphatic tube formation. YAP/TAZ are influenced by matrix stiffness,[59] and it was recently revealed that VEGF-C activates the Hippo signaling pathway,[23] which includes YAP/TAZ and their target genes, such as *MYC* and *CTGF*. PROX-1 expression is required for initial lymphatic specification and budding,[22] as well as for continued maintenance of a LEC phenotype,[60] and was recently revealed to be negatively regulated by YAP/TAZ.[23] Here, we show that the highest *PROX-1* expression corresponds to samples with the highest degree of tube formation, as expected based on previous findings, and that *TAZ* expression is inversely related. The trend for *YAP* remains less clear based on real time qRT-PCR results and shows the need to analyze individual cells and the spatial localization of YAP/TAZ. Upon quantification of YAP/TAZ expression in both the nuclei and cytoplasm, we observe significant degradation of both YAP and TAZ as substrate stiffness decreases, which aligns with PROX-1 upregulation and lymphatic budding. Conversely, when nucleic YAP/TAZ expression is upregulated, PROX-1 is inhibited and lymphatic maintenance occurs, which translates to no tube formation occurring in our HA-hydrogel system here (Figure 5D). It is important to note that there is no clear nuclear TAZ expression and that TAZ may be expressed independently of YAP. These observations seem to agree with previous reports that TAZ expression moves to the cytoplasm in the presence of Prox-1.[23] Additionally, when YAP/TAZ target genes, such as *MYC* and *CTGF* are downregulated in the presence of softer matrices, expression of PROX-1 targets such as VEGFR-3 and MMP-14 are also upregulated. Complementarily, exposure to soft matrices induces a GATA2-dependent increase in VEGFR-3 as well as LEC migration.[24] These mechanosensitive responses by LECs to substrate stiffness highlight the need for more physiologically relevant in vitro models in order to accurately elucidate mechanisms of action and also highlights the functionality of this HA-hydrogel system for future studies.[23]

Collectively, we show that by tuning both the matrix stiffness and VEGF-C concentration, the signaling pathways of lymphatic CLS formation can be regulated in a synthetic matrix. Findings from this simple 2D system will lay an important framework for future work in generating more complex lymphatic networks, which can be used for mechanistic studies and potentially as therapeutics for a range of lymphatic disorders.

CONFLICT OF INTEREST

The authors have declared that no conflict of interest exists.

AUTHOR CONTRIBUTIONS

L. Alderfer and D. Hanjaya-Putra conceived the ideas, designed the experiments, interpreted the data, and wrote the manuscript. L. Alderfer, E. Russo, A. Archilla, and B. Coe conducted the experiments and analyzed the data. All authors have approved the manuscript.

ORCID

Donny Hanjaya-Putra https://orcid.org/0000-0002-5403-544X

REFERENCES

1. Oliver G, Kipnis J, Randolph GJ, Harvey NL. The lymphatic vasculature in the 21st century: novel functional roles in homeostasis and disease. *Cell*. 2020;182:270-296.
2. Petrova TV, Koh GY. Biological functions of lymphatic vessels. *Science (80-)*. 2020;369:eaax4063.
3. Liao S, Padera TP. Lymphatic function and immune regulation in health and disease. *Lymphat Res Biol*. 2013;11:136-143.
4. Wang Y, Oliver G. Current views on the function of the lymphatic vasculature in health and disease. *Genes Dev*. 2010;24:2115-2126.
5. Dixon JB, Raghunathan S, Swartz MA. A tissue-engineered model of the intestinal lacteal for evaluating lipid transport by lymphatics. *Biotechnol Bioeng*. 2009;103:1224-1235.
6. Schaupper M, Jeltsch M, Rohringer S, Redl H, Holnthoner W. Lymphatic vessels in regenerative medicine and tissue engineering. *Tissue Eng Part B Rev*. 2016;22:395-407.
7. Helm C-L, Zisch A, Swartz MA. Engineered blood and lymphatic capillaries in 3-D VEGF-fibrin-collagen matrices with interstitial flow. *Biotechnol Bioeng*. 2006;96:167-176.
8. Marino D, Luginbühl J, Scola S, Meuli M, Reichmann E. Bioengineering dermo-epidermal skin grafts with blood and lymphatic capillaries. *Sci Transl Med*. 2014;6:221-234.
9. Muylaert DEP, Fledderus JO, Bouten CVC, Dankers PYW, Verhaar MC. Combining tissue repair and tissue engineering: bioactivating implantable cell-free vascular scaffolds. *Heart*. 2014;100.

10. Zhang L, Xu Q. Stem/progenitor cells in vascular regeneration. *Arterioscler Thromb Vasc Biol*. 2014;34:1114-1119.

11. Park KM, Gerecht S. Harnessing developmental processes for vascular engineering and regeneration. *Development*. 2014;141:2760-2769.

12. Hillel AT, Unterman S, Nahas Z, et al. Photoactivated composite biomaterial for soft tissue restoration in rodents and in humans. *Sci Transl Med*. 2011;3:93ra67.

13. Burdick JA, Prestwich GD. Hyaluronic acid hydrogels for biomedical applications. *Adv Mater*. 2011;23:H41-H56.

14. Faust HJ, Sommerfeld SD, Rathod S, et al. A hyaluronic acid binding peptide-polymer system for treating osteoarthritis. *Biomaterials*. 2018;183:93-101.

15. Toole BP. Hyaluronan: from extracellular glue to pericellular cue. *Nat Rev Cancer*. 2004;4:528.

16. Slevin M, Kumar S, Gaffney J. Angiogenic oligosaccharides of hyaluronan induce multiple signaling pathways affecting vascular endothelial cell mitogenic and wound healing responses. *J Biol Chem*. 2002;277:41046-41059.

17. Banerjee SD, Toole BP. Hyaluronan-binding protein in endothelial cell morphogenesis. *J Cell Biol*. 1992;119:643-652.

18. Xu X, Jha A, Harrington D, Farach-Carson M, Jia X. Hyaluronic acid-based hydrogels: from a natural polysaccharide to complex networks. *Soft Matter*. 2012;8:3280.

19. Prestwich G. Hyaluronic acid-based clinical biomaterials derived for cell and molecule delivery in regenerative medicine. *J Control Release*. 2011;155:193-199.

20. Wolf KJ, Kumar S. Hyaluronic acid: incorporating the bio into the material. *ACS Biomater Sci Eng*. 2019;5:3753-3765.

21. Banerji S, Ni J, Wang S-X, et al. LYVE-1, a new homologue of the CD44 glycoprotein, is a lymph-specific receptor for hyaluronan. *J Cell Biol*. 1999;144:789-801.

22. Wigle JT, Oliver G. An essential role for Prox1 in the induction of the LEC phenotype. *EMBO J*. 2002;21:1505-1513.

23. Hyunsoo C, Kim J, Ahn JH, et al. YAP and TAZ negatively regulate Prox1 during developmental and pathologic lymphangiogenesis. *Circ Res*. 2019;124:225-242.

24. Frye M, Taddei A, Dierkes C, et al. Matrix stiffness controls lymphatic vessel formation through regulation of a GATA2-dependent transcriptional program. *Nat Commun*. 2018;9:1511.

25. Hanjaya-Putra D, Yee J, Ceci D, Truitt R, Yee D, Gerecht S, et al. Vascular endothelial growth factor and substrate mechanics regulate in vitro tubulogenesis of endothelial progenitor cells. *J Cell Mol Med*. 2010;14:2436-2447.

26. Yee D, Hanjaya-Putra D, Bose V, Luong E, Gerecht S. Hyaluronic acid hydrogels support cord-like structures from endothelial colony-forming cells. *Tissue Eng Part A*. 2011;17:1351-1361.

27. Hanjaya-Putra D, Bose V, Shen Y-I, et al. Controlled activation of morphogenesis to generate a functional human microvasculature in a synthetic matrix. *Blood*. 2011;118:804-815.

28. Hanjaya-Putra D, Wong KT, Hirotsu K, et al. Spatial control of cell-mediated degradation to regulate vasculogenesis and angiogenesis in hyaluronan hydrogels. *Biomaterials*. 2012;33:6123-6131.

29. Vanderhooft JL, Alcoutlabi M, Magda JJ, Prestwich GD. Rheological properties of cross-linked hyaluronan-gelatin hydrogels for tissue engineering. *Macromol Biosci*. 2009;9:20-28.

30. Varberg KM, Winfree S, Chu C, et al. Kinetic analyses of vasculogenesis inform mechanistic studies. *Am J Physiol - Cell Physiol*. 2017;312(4):C446-C458. https://doi.org/10.1152/ajpcell.00367.2016

31. Wu M, Du Y, Liu Y, et al. Low molecular weight hyaluronan induces lymphangiogenesis through LYVE-1-mediated signaling pathways. *PLoS ONE*. 2014;9:e92857.

32. Lee KY, Mooney DJ. Hydrogels for tissue engineering. *Chem Rev*. 2001;101:1869-1880.

33. Nguyen EH, Daly WT, Le NNT, et al. Versatile synthetic alternatives to Matrigel for vascular toxicity screening and stem cell expansion. *Nat Biomed Eng*. 2017;1:96.

34. Lutolf MP, Hubbell JA. Synthetic biomaterials as instructive extracellular microenvironments for morphogenesis in tissue engineering. *Nat Biotechnol*. 2005;23:47-55.

35. Hanjaya-Putra D, Gerecht S. Vascular engineering using human embryonic stem cells. *Biotechnol Prog*. 2009;25:2-9.

36. Johnson LA, Prevo R, Clasper S, Jackson DG. Inflammation-induced uptake and degradation of the lymphatic endothelial hyaluronan receptor LYVE-1. *J Biol Chem*. 2007;282:33671-33680.

37. Makinen T, Veikkola T, Mustjoki S et al. Isolated lymphatic endothelial cells transduce growth, surival and migratory signals via the VEGF-C/D receptor VEGFR-3. *EMBO J*. 2001;20:4762-4773.

38. Kono T, Kubo H, Shimazu C, et al. Differentiation of lymphatic endothelial cells from embryonic stem cells on OP9 stromal cells. *Arterioscler Thromb Vasc Biol*. 2006;26:2070-2076.

39. Sweat RS, Sloas DC, Murfee WL. VEGF-C induces lymphangiogenesis and angiogenesis in the rat mesentery culture model. *Microcirculation*. 2014;21:532-540.

40. Campbell KT, Hadley DJ, Kukis DL, Silva EA. Alginate hydrogels allow for bioactive and sustained release of VEGF-C and VEGF-D for lymphangiogenic therapeutic applications. *PLoS ONE*. 2017;12:e0181484.

41. Varberg KM, Winfree S, Dunn KW, Haneline LS. Kinetic analysis of vasculogenesis quantifies dynamics of vasculogenesis and angiogenesis in vitro. *JoVE*. 2018;131:e57044. https://doi.org/10.3791/57044

42. Kazenwadel J, Secker GA, Betterman KL, Harvey NL. In vitro assays using primary embryonic mouse lymphatic endothelial cells uncover key roles for FGFR1 signalling in lymphangiogenesis. *PLoS ONE*. 2012;7:e40497.

43. Detry B, Bruyère F, Erpicum C, et al. Digging deeper into lymphatic vessel formation in vitro and in vivo. *BMC Cell Biol*. 2011;12:29.

44. Stratman AN, Saunders WB, Sacharidou A, et al. Endothelial cell lumen and vascular guidance tunnel formation requires MT1-MMP-dependent proteolysis in 3-dimensional collagen matrices. *Blood*. 2009;114:237-247.

45. Detry B, Erpicum C, Paupert J, et al. Matrix metalloproteinase-2 governs lymphatic vessel formation as an interstitial collagenase. *Blood*. 2012;119:5048-5056.

46. Van Hinsbergh VW, Engelse MA, Quax PH. Pericellular proteases in angiogenesis and vasculogenesis. *Arterioscler Thromb Vasc Biol*. 2006;26:716-728.

47. Kim J, Kim YH, Kim J, et al. YAP/TAZ regulates sprouting angiogenesis and vascular barrier maturation. *J Clin Invest*. 2017;127:3441-3461.

48. Mason DE, Collins JM, Dawahare JH, et al. YAP and TAZ limit cytoskeletal and focal adhesion maturation to enable persistent cell motility. *J Cell Biol*. 2019;218:1369-1389.

49. Grimm L, Nakajima H, Chaudhury S, et al. Yap1 promotes sprouting and proliferation of lymphatic progenitors downstream of Vegfc in the zebrafish trunk. *Elife*. 2019;8:e42881.

50. Gramolelli S, Cheng J, Martinez-Corral I, et al. PROX1 is a transcriptional regulator of MMP14. *Sci Rep*. 2018;8:9531.

51. Yao G, He P, Chen L, et al. MT1-MMP in breast cancer: induction of VEGF-C correlates with metastasis and poor prognosis. *Cancer Cell Int*. 2013;13:98.

52. Wong HLX, Jin G, Cao R, et al. MT1-MMP sheds LYVE-1 on lymphatic endothelial cells and suppresses VEGF-C production to inhibit lymphangiogenesis. *Nat Commun*. 2016;7:10824.

53. Lawrance W, Banerji S, Day AJ, Bhattacharjee S, Jackson DG. Binding of hyaluronan to the native lymphatic vessel endothelial receptor LYVE-1 is critically dependent on receptor surface clustering and hyaluronan organisation. *J Biol Chem*. 2016;291:8014-8030. https://doi.org/10.1074/jbc.M115.708305

54. Güç E, Briquez PS, Foretay D, et al. Local induction of lymphangiogenesis with engineered fibrin-binding VEGF-C promotes wound healing by increasing immune cell trafficking and matrix remodeling. *Biomaterials*. 2017;131:160-175.

55. Knezevic L, Schaupper M, Mühleder S, et al. Engineering blood and lymphatic microvascular networks in fibrin matrices. *Front Bioeng Biotechnol*. 2017;5:1-12.

56. Kriehuber E, Breiteneder-Geleff S, Groeger M, et al. Isolation and characterization of dermal lymphatic and blood endothelial cells reveal stable and functionally specialized cell lineages. *J Exp Med*. 2001;194:797-808.

57. Goldman J, Le TX, Skobe M, Swartz M. Overexpression of VEGF-C causes transient lymphatic hyperplasia but not increased lymphangiogenesis in regenerating skin. *Circ Res*. 2005;96:1193-1199.

58. Pulyaeva H, Bueno J, Polette M et al. MT1-MMP correlates with MMP-2 activation potential seen after epithelial to mesenchymal transition in human breast carcinoma cells. *Clin Exp Metastasis*. 1997;15:111-120.

59. Dupont S, Morsut L, Aragona M, et al. Role of YAP/TAZ in mechanotransduction. *Nature*. 2011;474:179-184.

60. Johnson NC, Dillard ME, Baluk P, et al. Lymphatic endothelial cell identity is reversible and its maintenance requires Prox1 activity. *Genes Dev*. 2008;22:3282-3291.

SUPPORTING INFORMATION

Additional Supporting Information may be found online in the Supporting Information section.